文章编号：1001－9014(2016)02－0194－06

DOI:10.11972/j.issn.1001－9014.2016.02.013

High efficiency conical shape THz coupler

CHEN Tian-Ji, HE Ting, ZHANG Bo, SHEN Jing-Ling*

(Beijing Key Laboratory for Terahertz Spectroscopy and Imaging, Key Laboratory of Terahertz Optoelectronics, Ministry of Education, Department of Physics, Capital Normal University, Beijing 100048, China)

Abstract: A coupler for coupling terahertz radiation into a waveguide was designed, which is the combination of a conical column and a short cylinder made of aluminum. The performance of the coupler in the cases of a broadband collimated terahertz wave and a single frequency collimated terahertz wave from free-space into an anti-resonate waveguide was simulated by theory and verified by experiment. The results confirm that the coupler is a high efficiency and broad band THz coupler. By optimizing the dimension parameters of the coupler, the amplitude coupling ratio of 71% and the amplitude concentration factor of 6.125 in the terahertz time domain spectroscopy system have been achieved.

Key words: terahertz coupler, conical aperture, waveguide

PACS: 07.57.Hm, 42.82.Et, 42.79.Gn

高效锥形太赫兹耦合器

陈天霁, 和 挺, 张 波, 沈京玲*

(首都师范大学 物理系 太赫兹光电子学教育部重点实验室, 北京 100048)

摘要: 设计了将太赫兹波耦合进入波导的耦合器. 耦合器由金属材料铝制成, 形状为中空圆锥形和圆柱形的结合. 在宽带的脉冲太赫兹信号和单频的连续太赫兹信号两种情况下, 模拟并实验测试了耦合器将自由空间传输的平行太赫兹波耦合进入反谐振波导, 结果显示该耦合器是宽带太赫兹波耦合器. 通过优化耦合器几何参数, 在太赫兹时域系统下得到振幅耦合率达到71%, 振幅增强因子为6.125.

关 键 词: 太赫兹耦合器; 锥形孔; 波导

中图分类号: TN252 **文献标识码**: A

Introduction

Terahertz radiation is the electromagnetic wave locating in the spectrum between infrared and microwave. In the past years, the terahertz technology has brought great progress in multitudinous applications in the fields of spectroscopy, imaging, biotechnology, communication, public security, chemical analysis, etc. In the THz applications THz waveguide is of importance for efficient THz transmission and has attracted many attentions. By now there are many works present diverse terahertz waveguides such as hollow metallic waveguide, parallel-plate waveguide, wire waveguide, dielectric waveguide, and photonic crystal fiber, etc.[1-9]. Among these waveguides, one of dielectric waveguides or anti-resonant waveguide as a sensor was reported by some literatures[10-14]. In our group Liu Jing used a 150 mm long anti-resonant waveguide to detect absorption spectrum of edible oil[12]. To reduce the transmission loss and improve signal to noise ratio and transmission efficiency of the waveguides a coupler coupling terahertz beam into waveguides is one of the solutions. In the past years some couplers to enhance terahertz transmission efficiency by different structures have been reported[15-24]. In 2012, M. Gerhard *et al.* coupled focused terahertz into a parallel plate waveguide by using a tapered structure, and got amplitude coupling ratio of 80%[15]. In 2013, Shuchang Liu *et al.* studied a conical aperture combination with a slit and found that the conical aperture or tapered structure can concentrate terahertz beam and the resulting transmission spectrum is a weighted sum of the spectra

Received date: 2015-02-01, **revised date**: 2015-12-24 **收稿日期**:2015-02-01, **修回日期**:2015-12-24

Foundation items: Supported by National Instrumentation Program (2012YQ140005), Nature Science Foundation of Beijing (4144069), and Science and Technology Project of Beijing Municipal Education Commission (KM201410028004)

Biography: CHEN Tian-Ji(1984-), Hubei province, master. Research area focus on terahertz waveguide. E-mail: 2120602022@cnu.edu.cn

* **Corresponding author**: E-mail: sjl-phy@cnu.edu.cn

associated with a tapered aperture with a slit[16]. In the same year they studied an array of tapered conical aperture, which can concentrate broadband terahertz (0.2 ~ 1T)[17]. Different coupler design may only fit a certain coupling demand. To increase terahertz signal coupling into the anti-resonant waveguide and get a broader band THz coupler, we designed and fabricated a coupler with the shape of a conical column combining with a short cylinder.

1 Design

The coupler was designed to work in two experimental systems. First, the incident terahertz wave is a pulsed collimated beam with 2 ps pulse length with frequency in the range of 0.2 ~ 2 THz , which is a common effective frequency range presented by a typical THz-TDS system. Second, the incident terahertz wave is a continuous collimated wave (CW) with the frequency of 3.1THz, which is presented by a terahertz CW laser. Although the coupler is designed to match a cylinder waveguide working in THz-TDS, we also hope that it can work in a CW system to improve imaging, communication and other aspects.

Besides, the following factors have been considered in our design. Firstly, coupling a pulsed signal needs to enhance the terahertz intensity in broadband. In a conventional THz-TDS system the effective bandwidth is usually about 2 THz and many samples' characteristic peaks locate in the range of 0.2 ~ 2 THz. So we simulated and designed the coupler worked in this frequency range, which is much broader than the previously work[16]. Secondly, the enhancing terahertz wave by the coupler should connect the waveguide closely, rather than the terahertz beam goes through a certain distance of free space as reported in reference[17], since terahertz beam usually be disturbed and lose energy in free space. Thirdly, instead of a silicon lens, by which only 20% ~ 30% coupling ratios can be achieved[15], a tapered structure is used to concentrate the terahertz beam for a high coupling ratios.

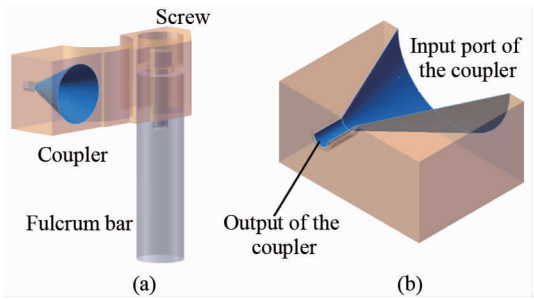

Fig. 1 (a) Assembling drawing of the coupler. The right part is used to fix the coupler, (b) The cross-section drawing of the coupler
图 1 (a) 耦合器的组装图,(b)耦合器的刨面图

Figure 1 (a) shows the coupler sketch we designed. The main functional structure is the combination of a conical column and a cylindrical column, and the cross-section is shown in Fig. 1(b). The conical part is used to concentrate terahertz wave from a thick beam to a slender beam, and the cylinder part is used to connect the following anti-resonant waveguide. Adapting to dimensions of the waveguide and the size of the terahertz beam, we selected lengths of the cylinder part and the conical part as 4 mm and 15 mm, inner and outer radii of the cylinder part as 1 mm and 1.5 mm, respectively. Clearly, the output port radius of the conical column is the same as that of the cylinder part. The inner radius of the input port of the conical column can be optimized by the simulation. Since the cylinder part connects the following waveguide conveniently and has not the function of beam concentration, the length of it was set as 4 mm, as short as possible. Being light, easy to be processed, and low cost, aluminum was chosen as the material of which the coupler was made. Moreover, as metal material aluminum is taken as a perfect conductor (reflector) and should realize broadband transmission.

2 Simulation

In order to understand the distribution of the THz field and to optimize the coupler, we simulated the transmission process of the THz beam and calculated the THz field distribution. The enhancement of terahertz electric field by the coupler and the transmission properties were studied using a two-dimensional axis symmetric finite element method (FEM) in the frequency domain. The rotational symmetry of the coupler makes it possible to set up a half sector plus a small rectangular in two dimensions as the simulation region, as shown in Fig. 2 (a). All the dimension parameters are labeled. The boundary is a perfect electric conductor. The simulation region is set as filled with air. The advantage of setting the model in 2D is much faster in calculation and saving memory in simulation. Since the coupler is made of aluminum, the boundary of the simulation region is set as perfect conductor. The inside region of the coupler is set as air. Considering two aspects, to couple more energy into the waveguide and the THz beam size (~ 13 mm), in the simulation we set the input port radius of the conical column in the range from 5 mm to 13 mm, and will get the best value of the radius according to the simulation results.

The performances of the coupler is shown in Figs. 2 (b), (c), and (d). Figure 2 (b) shows the terahertz amplitude distribution in the case of a pulsed THz wave, from which we can see that energy of terahertz field mainly distributes in the area of the rotational axis of the coupler and it is enhanced at the output port of the conical column.

To describe the coupling effect a terahertz amplitude concentration factor $f(r)$ is introduced, which is defined as

$$f(r) = A_{\text{out}}(r)/A_{\text{ref}} \quad , \quad (1)$$

where $A_{\text{out}}(r)$ is the amplitude of terahertz wave at the output port of the coupler and A_{ref} is terahertz amplitude at the same location without the coupler. Clearly, the $A_{\text{out}}(r)$ is the function of input port radius r and, therefore, the $f(r)$ is also the function of r. Figure 2 (c) shows the terahertz amplitude concentration factor $f(r)$ versus the radius of the input port of the coupler. In Fig. 2 (c) the black and red curves present $f(r)$ of a conical

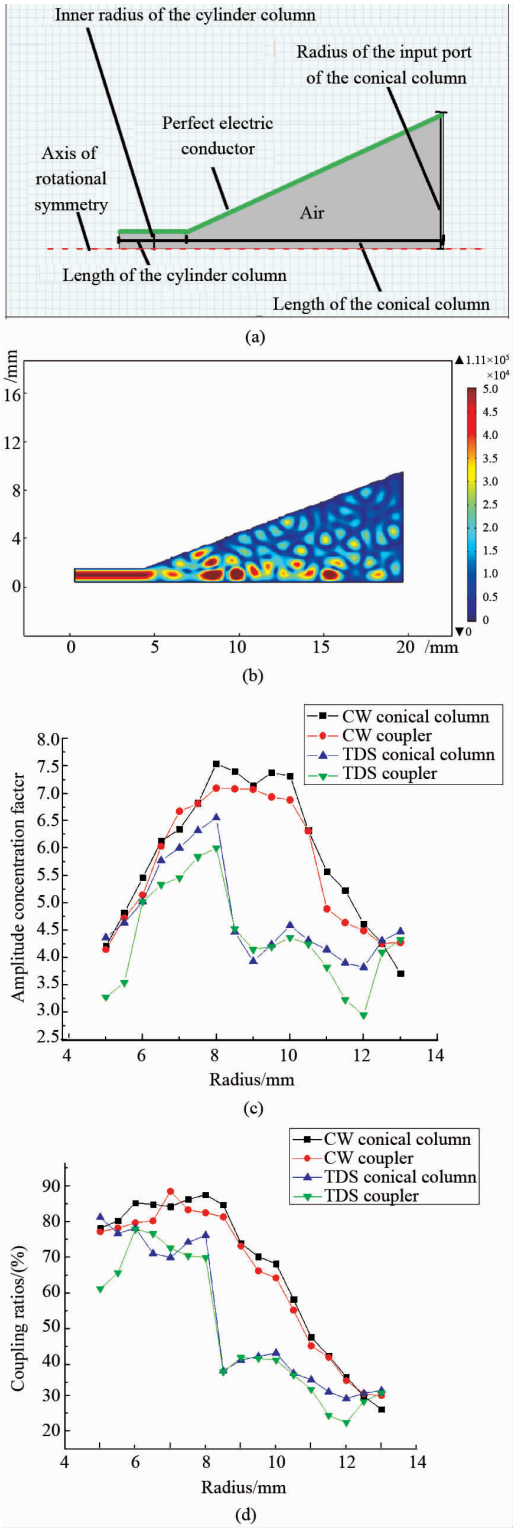

Fig. 2 (a) Simulation region, (b) terahertz field distribution by the simulation, (c) terahertz amplitude concentration factor versus the input port radius of the coupler, and (d) coupling ratio versus the input port radius of the coupler

图2 (a)仿真区域图,(b)仿真的太赫兹强度场分布,(c)太赫兹振幅增强因子和耦合器输入端半径的对应关系,(d)耦合效率和耦合器输入端半径对应关系

column itself and the coupler (a conical column plus a cylinder part), respectively, in the case of the input CW terahertz at 3.1 THz, and the blue and green curves present the $f(r)$ for the pulsed input terahertz beam. It is easy to see that the shapes of this two groups curves are different because the input THz beam in one case is pulsed and in the other is continuous wave. Nevertheless the changing tendencies of the curves are the same. The terahertz amplitude concentration factor $f(r)$ increases with the increase of the input port radius when the radius is small. However, when the radius is beyond a certain value, the $f(r)$ declines with the radius increasing. From the red and black curves it is shown that $f(r)$ is at a higher level (~ 7) with the r in the range from 8 mm to 10 mm. From the blue and green curves we find that $f(r)$ reaches its highest value (~ 6) at the radius of 8 mm. Since we hope the coupler works in both pulsed terahertz wave and continuous terahertz wave, we choose 8 mm as the input port radius of the coupler according to the results shown in Fig. 2 (c).

Another factor to describe the performance of the coupler is the coupling ratios which is defined as

$$C(r) = [A_{out}(r)/A_{in}(r)] \times 100\% \quad , \quad (2)$$

where $A_{out}(r)$ is the amplitude of THz wave at the output port and the $A_{in}(r)$ is the amplitude of terahertz wave at the input port. Figure 2 (d) presents the amplitude coupling ratios versus the radius of the input port of the coupler. We can see from Fig. 2 (d) that the amplitude coupling ratio remains a high level ($\sim 70\%$) when the input port radius is smaller than a certain value (8 mm), and it declines sharply when the radius is larger than 8 mm. These results are easy to understand. The smaller the input port radius is, the smaller the cone angle of the conical column is. There will be less terahertz energy flowing into the coupler. As the radius increases or the cone angle becomes larger, although the input terahertz beam still increase, more incident terahertz beam is held back, so the coupling ratio goes down. According to the result shown in Fig. 2 (d) we set the input port radius of the conical column in the range from 6 ~ 8 mm.

In consideration of both the concentration factor $f(r)$ and the coupling ratio $C(r)$ in terahertz TDS and CW by the simulation results shown in Fig. 2 (c) and Fig. 2 (d), we obtain the best input port radius of the coupler, which is 8 mm. Moreover, from Fig. 2 (c) and Fig. 2 (d) we can see that the curves of the conical column itself are almost above the curves of the coupler. Since the cylinder part does not have concentration function, the terahertz energy transmission slightly decline. The resulting transmission of the coupler is the sum of that passing through conical part and the cylinder part.

As mentioned above that terahertz amplitude mainly distributes in the area of the rotational axis of the coupler and a quasi-periodic distribution away from the output port can be observed from Fig. 2 (b). The distribution is discussed following. Due to the conical shape, which limits and changes the propagation direction of the incident THz beam, the beam in the conical column forms into two traveling terahertz beams after the process reaches a stable state. One propagates forwards from the input port to the output port, and the other propagates backwards. The two terahertz beams travel oppositely and

therefore a quasi-stationary wave forms. It leads to the amplitude of terahertz field enhanced nearby the cone vertex of the conical column. We call the position of the enhanced amplitude as terahertz field maximum position (TMP). By simulation we find out that the TMP is nearby the cone vertex and the TMP is mainly related to both the wavelength of the incident beam and the cone angle. Adjusting the input port radius of the conical column is equivalent to adjusting the cone angle. Optimizing the best radius actually make the TMP at the output port of the conical column to lead the most incident terahertz energy coupling into the following waveguide.

3 Experiment

We fabricated a coupler with aluminum by digital machining according to optimized parameters in the simulation. The coupler was tested in two experimental setups. One is a THz-TDS system, by which the incident terahertz wave is a pulsed beam with 2 ps pulse length and in 0.2 ~ 2 THz frequency range. The other is a THz-CW system, from which the incident terahertz beam is the continuous wave at the frequency of 3.1 THz. The schematic diagram of the experimental setups are shown in Figs. 3 (a) and (b). In Fig. 3(a) a collimated terahertz beam from PM3 is limited by an aperture and then enters into the coupler. We selectively used two apertures with different diameters: the bigger one with the radius the same as that of the input port of the coupler and the smaller one with the radius the same as that of the output port of it. The terahertz intensity is enhanced by the coupler and then travels through an anti-resonant waveguide. In Fig. 3(b) for THz-CW system, a collimated continuous terahertz beam (3.1 THz) goes in the coupler, then travels through the following anti-resonant waveguide just like in THz-TDS system. The temperature is 22 degree centigrade, and the relative humidity is 10% in the THz-TDS experiments.

The corresponding THz time-domain signals and frequency-domain signals are shown in Figs. 4 and 5. These spectra were measured in 6 different experimental configurations, which are shown in the small graphs at the bottom right in Fig. 4. To compare the effect of the coupler on the THz beam the time-domain curves in Fig. 4 are divided into 3 groups. Figure 4 (a) is in group 1, (b) ~ (d) in group 2, and (e) ~ (f) in group 3. Figure 4 (a) is the terahertz time domain signal traveling in free space, in the situation of no coupler, no aperture, and also no waveguide. Group 2, the curves in Figs. 4 (b) ~ (d) are the terahertz signals of traveling through a big aperture, a small aperture, and the coupler, respectively. The first two signals are taken as references for calculating the amplitude coupling ratio and the amplitude concentration factor, which will be explained in detail in following paragraphs. Group 3, the curves in Figs. 4(e) and (f) present the signals passing through an anti-resonant waveguide with or without the coupler.

The maximum value in the curves shown in Fig 5 was used to calculate the THz amplitude concentration factor and the coupling ratios according to Eqs. 1 and 2, and $f(r) = 6.125$ and $C(r) = 71\%$ are obtained, respectively. Due to the terahertz signal detection method,

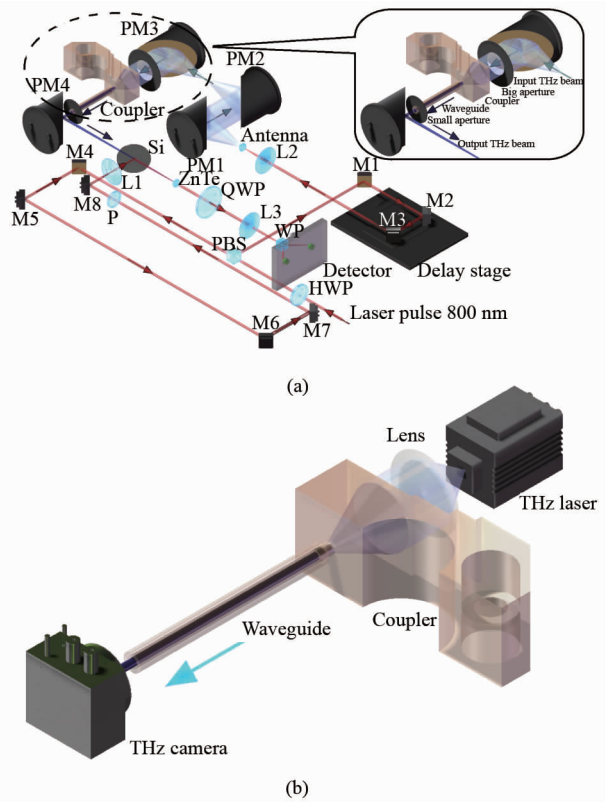

Fig. 3　The schematic diagram of the experimental setups (a) The terahertz time-domain spectroscopy system, the upper right is the local zoom in, and (b) the THz continuous wave system
图 3　实验系统原理图(a) 太赫兹时域光谱系统,右上角部分是耦合器的局部放大,(b) 太赫兹连续波系统

the $A_{in}(r)$ in Eq. 2 is actually measured as the terahertz signal passing through the big aperture. It is reasonable to do the replacement since the radius of the big aperture is the same as that of the coupler's input port, Fig. 4 (b), and the terahertz amplitude passing through the big aperture should be similar to $A_{in}(r)$. Due to the same reason, we used the terahertz signal passing through the small aperture as the reference A_{ref} in Eq. 1 to calculate the amplitude concentration factor. Considering the amplitude concentration factor and the coupling ratios are 6 and 73%, respectively, by the simulation, the experimental results are almost consistent with the simulation results.

Besides the above two factors to show the performance of the coupler, another important property can be observed in the experimental results shown in Figs. 4 and 5, that is, it is a broad band coupler. This means that the coupler dose enhance the terahertz intensity and has little negative affection on the spectrum. It also shows that the shapes of the terahertz signals through the waveguide with and without the coupler are nearly the same from the group3, Figs. 4 (e) ~ (f). This performance of the coupler is especially obvious by seeing in frequency domain spectrum, for each spectrum the corresponding peaks are almost at the same frequency. This smooth terahertz intensity concentration performance is very important for terahertz spectral applications.

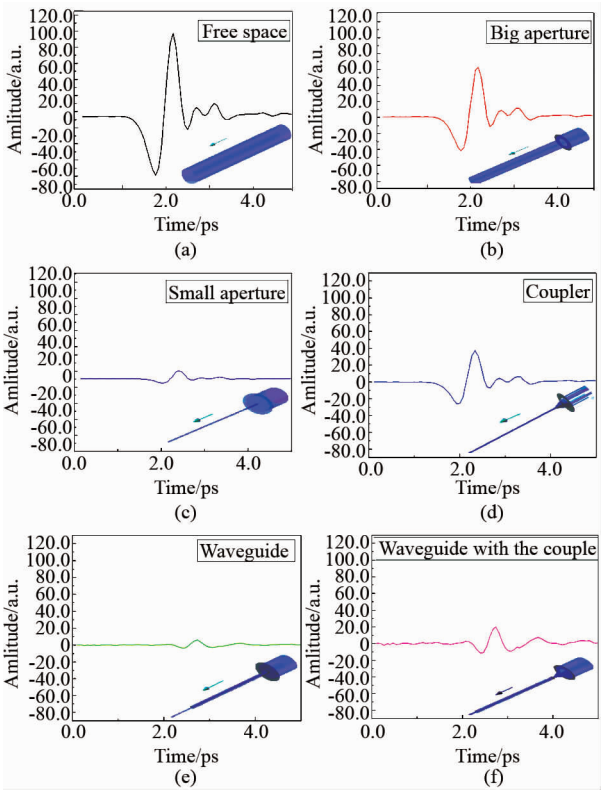

Fig. 4 Terahertz time-domain signals in various situations. The inserts in the bottom right present the visual view of the 6 situations of the THz beam around the place to insert the coupler. (a) The terahertz beam propagates in free space, (b) the terahertz beam is limited by the big aperture, (c) the terahertz beam limited by the small aperture, (d) the terahertz beam travels through the coupler, (e) the terahertz beam goes through the anti-resonant waveguide without the coupler, and (f) the terahertz beam goes through the anti-resonant waveguide with the coupler

图4 不同情况下的太赫兹时域光谱. 每幅图右下角插入的小图表示太赫兹光速经过耦合器或者对应位置时的实际情况. (a)自由空间中的太赫兹光束,(b)太赫兹光束只被一个大孔径光阑限制,(c) 太赫兹光束只被一个小口径光阑限制,(d)经过耦合器的太赫兹光束,(e)没有耦合器时经过波导的太赫兹光束,(f)通过耦合器后,再经过波导的太赫兹光束

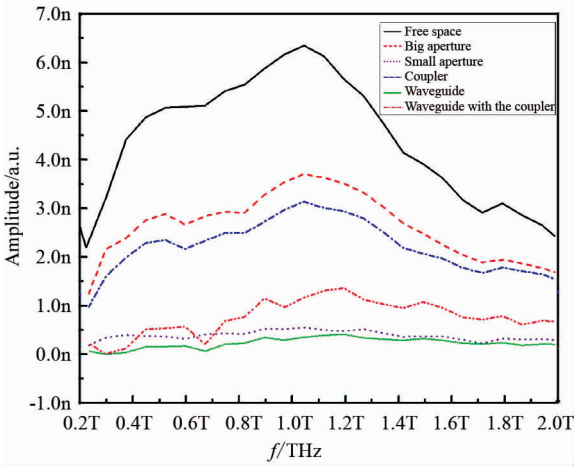

Fig. 5 Frequency-domain signals of the relevant time-domain signals in Fig. 4

图5 图4中的时域光谱对应的频域光谱

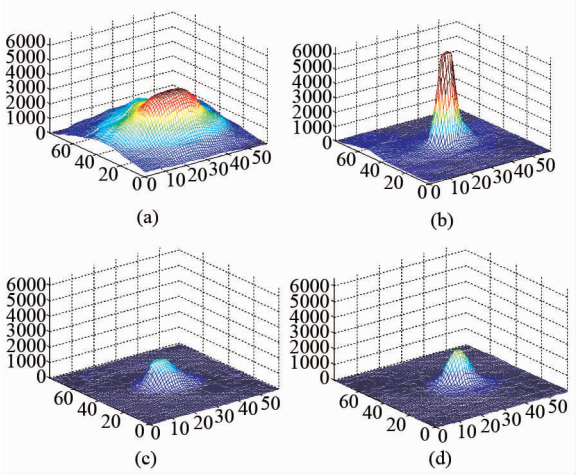

Fig. 6 Terahertz intensity distribution in THz CW experiment. (a) Free space, (b) terahertz signal passing through the coupler, (c) the singal passing through a waveguide without the coupler, and (d) the signal passing through a waveguide with the coupler

Fig. 6 在连续太赫兹系统中,太赫兹强度分布图. (a)自由空间的太赫兹分布,(b)通过耦合器的太赫兹强度分布,(c)没有耦合器时,通过波导的太赫兹分布,(d)经由耦合器后,通过波导的太赫兹分布

The corresponding experimental results by the THz-CW system are shown in Fig. 6, in which the terahertz intensity distributions detected by the Pyroelectric Array Camera (Pyrocam™ III) are plotted in the cases of free space (a), the coupler (b), and the waveguide with (c) or without (d) the coupler. From Fig. 6 we can see that the coupler does enhance the terahertz intensity or couple more terahertz energy into the waveguide. It can also been seen that the mode distribution both in the coupler and in the waveguide with the coupler is HE_{11}.

4 Conclusions

We have designed a coupler for THz cylinder waveguides structured as a conical column and a cylindrical column and simulated the properties for both the pulsed collimated wave in the frequency of 0.2 ~ 2 THz and the continue collimated wave at 3.1 THz. The parameters of the coupler is optimized by the simulation and the best radius of the input port of the coupler, 8 mm, is obtained. The performance of the coupler is demonstrated on the two experimental systems, THz-TDS and THz-CW. With the desinged parameters the amplitude coupling ratios of 71% and the concentration factor of 6.125 are achieved by the coupler. The results indicate that the coupler we fabricated can be used to couple the THz wave into a waveguide. The high coupling efficiency coupler is very important for the implementation of waveguides.

Acknowledgements

This work was supported by the National Instrumentation Program (Grant no. 2012YQ140005), the Nature Science Foundation of Beijing (Grant No. 4144069) and Science and Technology Project of Beijing Municipal Education Commission (Grant No. KM201410028004).

References

[1] Zhao C F, Huang B, Shi Z S. Characteristic equation method for propagation properties of terahertz wave in circular hollow waveguide [J]. *Journal of Xi' an Jiaotong University*, 2012, **46**(6): 12 - 17.

[2] Bang S S, Xiao L T, Xuan Z, *et al*. Characterization of cylindrical terahertz metallic hollow waveguide with multiple dielectric layers [J]. *Appl. Opt.* 2012, **51**(30): 7276 - 7285.

[3] Rajind M, Victoria A, Liu J, *et al*. Terahertz microfluidic sensor based on a parallel-plate waveguide resonant cavity [J]. *Appl. Phys. Lett.* 2009, **95**: 171113.

[4] Zhan H, Mendis R, Mittleman D M. Superfocusing terahertz waves below λ/250 using plasmonic parallel-plate waveguides [J]. *Opt. Express*. 2010, **18**(9): 9643 - 9650.

[5] Mbonye M, Mendis R, Mittleman D M. A terahertz two-wire waveguide with low bending loss [J]. *Appl. Phys. Lett*. 2009, **95**: 233506.

[6] Pahlevaninezhad H, Darcie E T, Heshmat B. Two-wire waveguide for terahertz [J]. *Opt. Express* 2010, **18**(7): 7415 - 7420.

[7] Hu J, Chen H. Loss characteristics of photonic crystal fiber as terahertz waveguide [J]. *Chinese J. Lasers*. 2008, **35**(4): 568 - 571.

[8] Shchurova L Y, Namiotb V A. On generation of electromagnetic waves in the terahertz frequency range in a multilayered open dielectric waveguide [J]. *Phys. Lett. A*. 2013, **377**: 2440 - 2446.

[9] You B, Chen H Z, Lu J Y, *et al*. Terahertz anti-resonant reflecting hollow waveguide sensor [C]. *In Lasers and Electro-Optics and Quantum Electronics and Laser Science Conference*, San Jose, CA, USA: 2010.

[10] You B, Lu J Y, Liou J H, *et al*. Subwavelength film sensing based on terahertz anti-resonant reflecting hollow waveguides [J]. *Opt. Express*. 2010, **18**(18): 19353 - 19360.

[11] Nguema E, Férachou D, Humbert G, *et al*. Broadband terahertz transmission within the air channel of thin-wall pipe [J]. *Opt. Lett.* 2011, **36**(10): 1784.

[12] Liu J. *Study of terahertz anti-resonant polymer waveguide. Master thesis* [M], Capital Normal University, 2014.

[13] Xiao M F, Liu J, Zhang W, *et al*. THz wave transmission in thin-wall PMMA pipes fabricated by fiber drawing technique [J]. *Opt. Commun*. 2013, **298**: 101 - 105.

[14] Xiao M F, Liu J, Zhang W, *et al*. Self-supporting polymer pipes for low loss single-mode THz transmission [J]. *Opt. Express*. 2013, 21 **17**: 19808 - 19815.

[15] Gerhard M, Theuer M, Rahm M, *et al*. High efficiency coupling into tapered parallel plate terahertz waveguides [C]. *In Conference on Lasers and Electro Optics - Far infrared or terahertz and Guided waves*, San Jose, CA, USA: 2013.

[16] Liu S C, Mitrofanov O, Nahatal A. Transmission bleaching and coupling crossover in a split tapered aperture [J]. *Opt. Express*. 2013, **21**(25): 30895 - 30902.

[17] Liu S C, Vardeny Z V, Nahata1 A. Concentration of broadband terahertz radiation using a periodic array of conically tapered apertures [J]. *Opt. Express*. 2013, **21**(10): 12363 - 12372.

[18] Gerhard M, Theuer M, Beigang R. Coupling into tapered metal parallel plate waveguides using a focused terahertz beam [J]. *Appl. Phys. Lett*. 2012, **101**: 041109.

[19] Zeng X H, Fan Z Y, Zhou P. Field distributions and transmission property inside a conical waveguide with a sub-wavelength-sized exit hole [J]. *Acta. Optica. Sinica*. 2009; **29**(6): 1488 - 1492.

[20] Kim S H, Lee E S, Ji Y B, *et al*. Improvement of THz coupling using a tapered parallel-plate waveguide [J]. *Opt. Express*. 2010, **18**(2): 25441 - 25448.

[21] Nguyen T D, Vardeny Z V, Nahata A. Concentration of terahertz radiation through a conically tapered aperture [J]. *Opt. Express*. 2010, **18**(24): 25441 - 25448.

[22] Theuer M, Shutler A J, Harsha S S, *et al*. Terahertz two-cylinder waveguide coupler for transverse-magnetic and transverse-electric mode operation [J]. *Appl. Phys. Lett*. 2011, **98**: 071108.

[23] Peytavit E, Lampin J F, Akalin T, *et al*. Integrated terahertz TEM horn antenna [J]. *Electron Lett*. 2007, **43**(2): 73 - 75.

[24] Armand D, Taniguchi H, Kadoya Y, *et al*. Terahertz full horn-antenna characterization [J]. *Appl. Phys. Lett*. 2013, **102**: 141115.